Downloaded 09/01/18 to 24.4.136.208. Redistribution subject to SEG license or copyright; see Terms of Use at http://library.seg.org/

Predicted and observed shear on pre-existing faults during hydraulic fracture stimulation

Mark D. Zoback and Jens-Erik Lund Snee, Stanford University Department of Geophysics*

Summary

Multi-stage hydraulic fracturing increases production from extremely low-permeability unconventional reservoirs by simultaneously inducing slip on pre-existing fracture planes. Here we illustrate how the high pore pressure generated during hydraulic fracturing operations induces slip on pre-existing fractures and faults with a wide range of orientations, thus creating an interconnected permeable fracture network. We demonstrate the basic principles of stimulating slip on poorly oriented faults using the stress state for a horizontal well in the Barnett Shale where fracture orientation data are also available from an image log. We compare this analysis with independent fracture orientation data obtained from earthquake focal plane mechanisms. Using the stress data, we are able to determine which nodal plane slipped in each microseismic event. As the two analyses yield essentially identical results, they show the basic processes by which slip on planes of varied orientations occurs during hydraulic stimulation. We extend this analysis to address some misconceptions about the likelihood of slip on horizontal bedding planes and planes parallel and perpendicular to horizontal principal stress directions. Notably, we show that inducing slip on horizontal or sub-horizontal bedding planes is nearly impossible except in compressive (reverse to strike-slip/reverse) stress states ($S_{\mathrm{Hmax}} \geq S_{\mathrm{hmin}} \approx S_{\mathrm{V}}$) or when ambient pore pressure is extremely high. The latter case results in very small differences in the magnitudes of the three principal stresses, regardless of the regional stress state.

Introduction

While it is generally accepted that the microseismic events that accompany multi-stage hydraulic fracturing in horizontal wells principally result from shear slip on pre-existing fractures and faults, the relationships among fracture orientation, the state of stress, and the pore pressure perturbation caused by hydraulic fracturing is often poorly understood. For example, questions are sometimes hotly debated regarding how slip occurs on planes with highly varied orientations, whether some microseismic events are associated with bedding plane slip and/or opening mode deformation, and whether the subsurface fracture distributions can be characterized by orthogonal fracture sets aligned with current stress directions. In this paper, we investigate the relationships between the state of stress, slip on pre-existing fractures, and pore pressure using a unique dataset from Barnett Shale that is illustrated in Figure 1. We then generalize this discussion to other stress states.

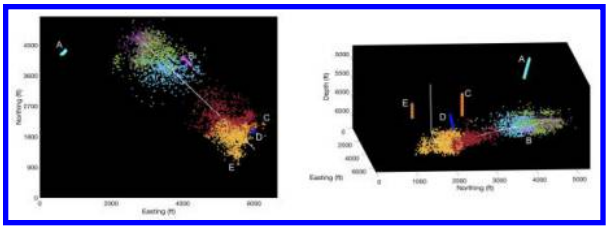

Figure 1: Perspective view of microseismic events generated during multistage hydraulic fracturing in the Barnett Shale. Dots are colored by stage number. Triangles labeled A–E represent the locations of seismometers in multiple down-hole monitoring arrays. Two arrays were active at a time during fracturing operations.

Summary of dataset

The microseismic dataset was acquired in a fairly routine manner. Twenty-level, 3-component seismometer arrays were sequentially deployed in 4 near-vertical wells and one horizontal well (labeled A–E in Figure 1), when 5 hydraulic fracturing stages were stimulated in the horizontal well shown. The microseismic events associated with each stage were recorded by at least two arrays. Although the relative locations of these events were poorly constrained (see Hakso and Zoback, 2017), Kuang et al. (2017) carried out a detailed analysis of the seismic waveforms to obtain focal plane mechanisms associated with each stage. Inversion of the focal plane mechanisms associated with each stage yielded very similar strike-slip/normal faulting stress states, with the maximum horizontal stress (S_{Hmax}) trending NE–SW. This stress state is essentially identical to that determined from hydraulic fracturing and other information (Hakso, 2017).

This dataset also includes orientations of pre-existing fractures measured with a Formation Microimager (FMI) image log run prior to stimulation. The orientations of pre-existing fractures are shown in the stereonets of Figure 2. Only one of the two nodal planes associated with each focal plane mechanism represents the orientation of the fault that actually slipped. The other nodal plane, the auxiliary plane, has no physical significance. Kuang et al. (2017) identified the active fault from the microseismic focal mechanisms by selecting the nodal plane with the higher Coulomb failure function (CFF), representing the plane that would be most likely to slip in the ambient stress field, defined as:

$$CFF = \tau - \mu\sigma_n,$$

where τ and σ_n are the shear and effective normal stresses resolved on the fault, respectively, and μ is the fault's coefficient of friction. Having both the information about pre-existing faults from the image log as well as the planes

© 2018 SEG

10.1190/segam2018-2991018.1

Downloaded 09/01/18 to 24.4.136.208. Redistribution subject to SEG license or copyright; see Terms of Use at http://library.seg.org/

that actually slipped, we can compare predictions of plane orientations that *should* slip with those that *actually* slipped as microseismic events.

Kuang et al. (2017) report an S_{Hmax} orientation of N053ºE based on an *in situ* measurement made in a nearby wellbore. This is consistent with several S_{Hmax} orientations measured *in situ* by Lund Snee and Zoback (2016) that range between N020ºE–N055ºE from within 30 km of the present study. Lund Snee and Zoback (2016) also mapped a normal/strike-slip faulting regime in this area, with $S_{\mathrm{V}} \geq S_{\mathrm{Hmax}} > S_{\mathrm{hmin}}$, where S_{V} is the vertical principal stress and S_{hmin} is the minimum horizontal principal stress. These *a priori* constraints are consistent with the results of stress inversions conducted by Kuang et al. (2017). Using their microseismic focal mechanisms, they found a normal/strike-slip faulting regime and an S_{Hmax} orientation of N060ºE.

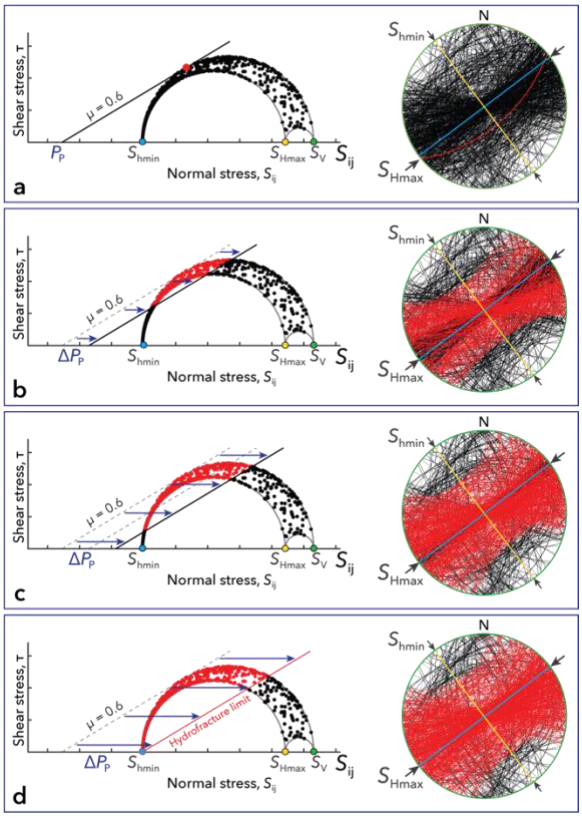

Figure 2: Mohr circles and stereonet plots illustrating the natural fractures measured in the FMI log that would be active at progressively increasing pore pressures during stimulation. a.–c. The number of fractures that will potentially fail in shear (red planes) increases as the pore pressure perturbation (ΔP_{P}) increases. d. The fractures that are expected to slip once P_{P} reaches the frac gradient ("Hydrofrac limit").

Predicted orientations of fractures that experienced shear failure

Figure 2 shows the orientations of fractures measured in the FMI log for the entire logged portion of the well in two ways. The plots on the left are Mohr diagrams normalized by the vertical stress, which illustrate the shear and normal stresses resolved on each plane in the measured stress state. The plots on the right are stereonets, which provide a geometrical view of the plane orientations in space. Hypothetical planes perpendicular to S_{V}, S_{Hmax}, and S_{hmin} are shown in green, yellow, and blue, respectively, for visualization purposes. Planes colored red represent fractures that are critically stressed ($CFF \geq 0$) under the pore pressure (P_{P}) and stress conditions shown in each plot.

Note that the Mohr diagrams shown here are presented in terms of total stress, rather than effective stress. Presentation in this way makes the intercept of the Coulomb frictional failure line with the abscissa equal to the ambient pore pressure. Ignoring poroelastic stress changes, which are likely to be quite small in relatively impermeable formations pressurized for short periods of time, we can thus evaluate the tendency for slip by simply displacing the friction line to the right to represent ever-increasing pore pressure. In general, the physical limit to the amount that pore pressure can be raised is the least principal stress.

Brittle rocks in the Earth's crust are critically stressed, meaning that the faults best oriented for slip within the ambient stress field are in a state of frictional equilibrium. Other ways of saying this are that the frictional strength of well-oriented faults limits stress magnitudes and/or that the shear stress on well-oriented faults are within one earthquake stress drop of frictional failure (Zoback et al., 2002). This condition is represented by the red plane shown in Figure 2a, which is the fracture measured in the image log that is best oriented for slip under the stress field constraints that we describe above. Figure 2a represents the stress and pore pressure conditions that exist prior to stimulation, assuming for visualization purposes (but not by necessity) that pore pressure is approximately hydrostatic and that the fracture best oriented for slip was exactly critically stressed ($CFF = 0$) at the start of stimulation. Figures 2b, 2c, and 2d show cases during stimulation in which the fluid injection progressively increases until it reaches the frac gradient ($P_{\mathrm{P}} \approx S_{\mathrm{hmin}}$) in Figure 2d ("hydrofracture limit"). For illustration, we neglect "net pressure," the amount that the pressure exceeds the least principal stress during high-rate pumping of a viscous fluid. This is typically on the order of a few MPa (a few hundred psi).

As pressure increases, more and more poorly oriented planes begin to slip (the dots in the Mohr diagrams and planes in the stereonets change from black to red). This illustrates the

© 2018 SEG

10.1190/segam2018-2991018.1

Downloaded 09/01/18 to 24.4.136.208. Redistribution subject to SEG license or copyright; see Terms of Use at http://library.seg.org/

critical importance of the process of shear stimulation during slickwater hydraulic fracturing. Many "old, dead" fractures and faults are stimulated in shear, become permeable, and their highly variable orientations result in an interconnected fracture network. Note that once the frac gradient is reached, the majority of planes are expected to slip, but many will not; as explained below, these are the planes that are roughly perpendicular to the vertical stress (planes with low dip) or S_{Hmax} (planes with steep dip that strike NW–SE).

Comparison with orientations of fractures that slipped during stimulation

The discussion above is presented in the context of the actual stress state for the Barnett well, as well as fractures observed with an image log in the well. This said, it is only a heuristic discussion in that we offered no proof that those planes actually slipped. However, because we know the focal plane mechanisms of these events and the planes that slipped in the microearthquake sequence, we compare in Figure 3 the planes we presumed to slip in Figure 2d with those that actually slipped. Note the overall consistency of Figures 3a and 3b. The planes shown in Figure 3b *did* slip and are quite similar to the planes *expected* to slip based on the available fault population seen in the image log.

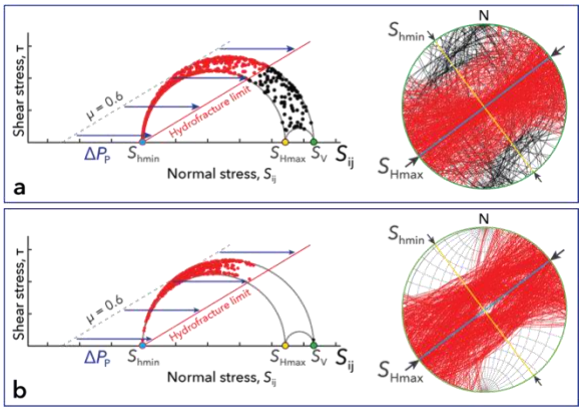

Figure 3: a. Plots showing the fractures identified in the FMI log. Planes colored red would be expected to slip during stimulation at pore pressures sufficient to propagate a hydraulic fracture. b. Plots of the orientations of planes that actually slipped during stimulation. These orientations were generated by sampling from a distribution of active faults from microseismic focal mechanisms with noise applied to represent orientation uncertainties.

Importance of the stress state

It is obvious that the nature of shear stimulation illustrated in the figures above is dependent on the orientations of the fractures and faults that are present, the stress state, and the fluid pressure perturbation. To illustrate the importance of the stress state, in Figure 4 we revisit the case considered in Figure 2, keeping the everything the same except the stress state. Instead of a normal/strike-slip faulting stress state ($S_{hmin} \ll S_{Hmax} \approx S_V$) typical of the Fort Worth Basin, we consider a strike-slip/reverse faulting stress state representative of parts of the Appalachian and Alberta basins ($S_{hmin} \approx S_V \ll S_{Hmax}$). Coincidentally, the S_{Hmax} orientation in all three areas is approximately NE–SW. While there are many similarities between Figures 2 and 4, with moderate increases in pore pressure in Figure 4b only strike-slip faults (very steeply dipping faults striking ±30° from the S_{Hmax} direction) are made to slip. At higher pressures (Figures 4c and 4d), slip is expected on many planes, some at very high angle to S_{Hmax} and some sub-horizontal.

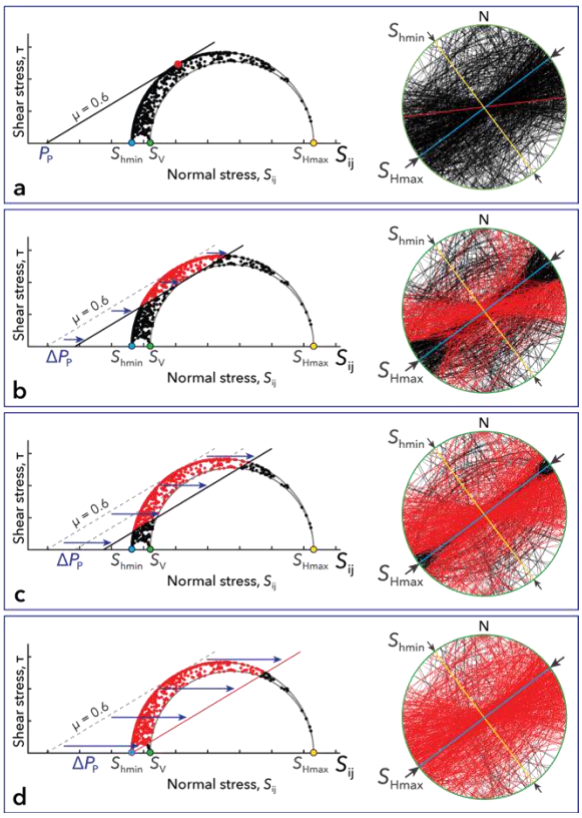

Figure 4: Mohr diagrams and stereonets showing which planes would be expected to slip if stimulation had instead occurred in a strike-slip/reverse faulting stress state.

Slip and opening on sub-horizontal bedding planes and near-vertical fractures striking sub-parallel to S_{Hmax}?

A number of publications hypothesize that slip and/or opening occur on sub-horizontal bedding planes and/or near-vertical fractures striking sub-parallel to the direction of S_{Hmax}. This is illustrated in Figure 5. At the left, a hypothetical focal plane mechanism is shown that implies

© 2018 SEG

10.1190/segam2018-2991018.1

Downloaded 09/01/18 to 24.4.136.208. Redistribution subject to SEG license or copyright; see Terms of Use at http://library.seg.org/

either that dip slip (west side up) occurred on a near-vertical plane striking approximately N–S, or that slip occurred on an orthogonal horizontal (presumably bedding) plane (rock above the bedding plane moving to the east). This is illustrated in the cross-section in the center. The possibility of opening-mode deformation is shown schematically on the right. Of course, it is theoretically possible for both slip and opening to occur on the same plane.

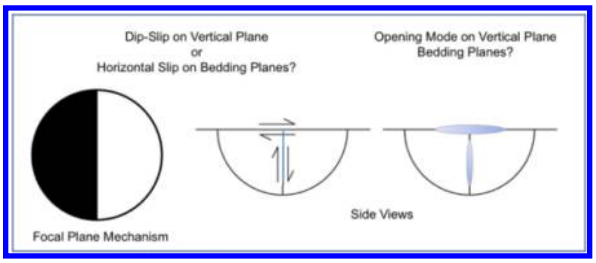

Figure 5: Illustration of the focal plane mechanism that would be produced by slip on a horizontal or vertical plane.

Despite the heated discussions surrounding this topic, one can extend the analysis illustrated in Figures 2–4 to address this. Recall that in terms of the Coulomb criterion, for slip to occur on a plane the CFF must increase to zero. Another way of saying this in terms of the Mohr diagrams shown above is that the point representing a potential slip plane must touch the frictional failure line. Similarly, for opening-mode deformation to occur, the effective normal stress on the fault must be less than zero. Another way of saying this is that a point representing a potential opening plane must be to the left of the intersection of the frictional failure line with the abscissa. Figure 6 shows how these conditions might be met in the two stress states considered above in Figures 2d and 4d. For a normal/strike-slip faulting stress state, Figure 6a demonstrates that it is essentially impossible to cause either planes sub-parallel to gently-dipping bedding or normal to S_{Hmax} (the green and yellow circles, respectively) to slip (or open), even when pore pressure reaches the magnitude of the least principal stress. In a strict sense, this also true for planes sub-parallel to S_{hmin} (blue circle), recognizing that during hydraulic stimulation, the net pressure can be a few MPa (a few hundred psi) above the least principal stress. In terms of Figure 6a, the frictional failure line would shift slightly to the right, making it possible for both the slip criterion and opening mode criterion to be satisfied. Hence, in a normal/strike-slip stress environment, it is possible for both shear and opening of fractures and faults sub-parallel to hydraulic fractures when the pumping pressure slightly exceeds S_{hmin}. The situation is completely different in the strike-slip/reverse faulting stress state shown in Figure 6b. When net pressure results in pressures reaching values slightly in excess of S_{hmin}, it would be possible for opening and shear to occur on planes sub-parallel to hydraulic fractures, but slip might also occur on sub-horizontal planes, depending on the difference in the magnitude of S_{hmin} and S_{V}, and the magnitude of the net pressure. However, just like the normal/strike-slip stress state, it is essentially impossible for slip (or opening) to occur on planes approximately normal to S_{Hmax}.

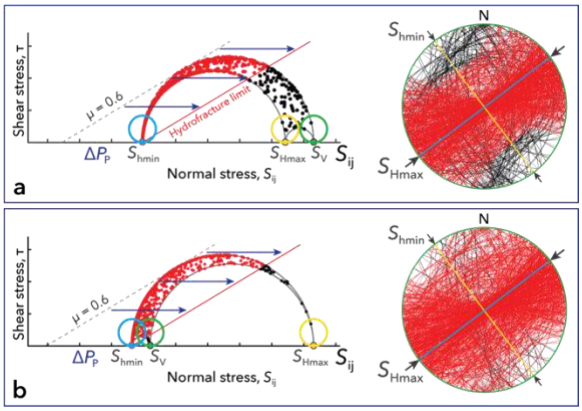

Figure 6: Evaluation of the tendency for shear slip or opening on planes normal to one of the principal stresses. Sub-horizontal bedding planes are illustrated by the green dot on left and the plane shown in green on the stereonet. Planes normal to S_{hmin} (sub-parallel to hydraulic fractures) are shown in blue and those normal to S_{Hmax} are shown in yellow. a. The normal/strike-slip stress state ($S_{\mathrm{hmin}} \ll S_{\mathrm{Hmax}} \approx S_{\mathrm{V}}$) considered in Figure 2d. b. The strike-slip/reverse stress state considered in Figure 4d ($S_{\mathrm{hmin}} \approx S_{\mathrm{V}} \ll S_{\mathrm{Hmax}}$).

Summary

The simple analyses presented here demonstrate the importance of prior constraints on the stress field and the orientation of pre-existing fractures and faults to estimate which planes can be made to slip during stimulation. Reliable predictions of the active fractures enable one to construct realistic discrete fracture network models and estimate the total stimulated rock value that might be accessed during hydraulic fracturing according to specified stimulation strategies. Such predictions can be fed into testable models and improved iteratively as additional data become available during continued operations to optimize the success of stimulation.

Acknowledgements

We thank Total for providing the data used in this analysis. This research was supported by the Stanford Natural Gas Initiative (NGI).

© 2018 SEG

10.1190/segam2018-2991018.1

REFERENCES

Hakso, A., 2017, Analysis of microseismic multiplets in a hydraulic fracturing operation: Ph.D. thesis, Stanford University.

Hakso, A., and M. D. Zoback, 2017, Using multiplets as an independent assessment of relative microseismic location uncertainty. The Leading Edge, **36**, 829–836, https://doi.org/10.1190/tle36100829.1.

Kuang, W., M. D. Zoback, and J. Zhang, 2017, Estimating geomechanical parameters from microseismic plane focal mechanisms recorded during multistage hydraulic fracturing: Geophysics, **82**, no. 1, KS1–KS11, https://doi.org/10.1190/GEO2015-0691.1.

Lund Snee, J.-E., and M. D. Zoback, 2016, State of stress in Texas: Implications for induced seismicity: Geophysical Research Letters, **43**, 10,208–10,214, https://doi.org/10.1002/2016GL070974.

Zoback, M. D., J. Townend, and B. Grollimund, 2002, Steady-state failure equilibrium and deformation of intraplate lithosphere: International Geology Review, **44**, 383–401, https://doi.org/10.2747/0020-6814.44.5.383.

Downloaded 09/01/18 to 24.4.136.208. Redistribution subject to SEG license or copyright; see Terms of Use at http://library.seg.org/